LUND UNIVERSITY

The FERRUM project: metastable lifetimes in Cr II

Backstrom, E.; Gurell, J.; Royen, P.; Mannervik, S.; Norlin, L.; Blackwell-Whitehead, Richard; Hartman, Henrik; Nilsson, Hampus

Link to publication

The FERRUM project: metastable lifetimes in Cr II

E. Bäckström,[1]⋆ J. Gurell,[1] P. Royen,[1] S. Mannervik,[1] L. Norlin,[2] R. Blackwell-Whitehead,[3] H. Hartman[3] and H. Nilsson[3]

[1]*Department of Physics, AlbaNova University Center, Stockholm University, SE-106 91 Stockholm, Sweden*
[2]*Department of Nuclear Physics, AlbaNova University Center, Royal Institute of Technology, SE-106 91 Stockholm, Sweden*
[3]*Lund Observatory, Lund University, Box 43, SE-221 00 Lund, Sweden*

ABSTRACT

Parity forbidden radiative transitions from metastable levels are observed in spectra of low-density astrophysical plasmas. These lines are used as probes of the physical conditions, made possible due to the long lifetime of their upper level. In a joint effort, the FERRUM project aims to obtain new and accurate atomic data for the iron-group elements, and part of this project concerns forbidden lines. The radiative lifetimes of the metastable energy levels $3d^4(a^3D)4s\ c^4D_{5/2}$ and $3d^4(a^3D)4s\ c^4D_{7/2}$ of singly ionized chromium have been measured. The experiment has been performed at the ion storage ring CRYRING. We employed a laser-probing technique developed for measuring long lifetimes. In this article, we present the lifetimes of these levels to be $\tau_{5/2} = 1.28(16)\,\mathrm{s}$ and $\tau_{7/2} = 1.37(7)\,\mathrm{s}$, respectively. A comparison with previous theoretical work shows good agreement and the result is discussed in a theoretical context.

Key words: atomic data – methods: laboratory – techniques: spectroscopic – astronomical data bases: miscellaneous.

1 INTRODUCTION

The FERRUM project (Johansson et al. 2002) is an international collaboration which aims to obtain new and accurate atomic data of the group of iron-peak elements, which runs from Sc to Cu in the periodic table. The spectra of these elements are intrinsically rich because of their complex energy-level structure, arising from the open 3d-shell. The dense level structure makes theoretical modelling of these elements difficult where different approaches may produce different results (Fischer 2009). Experimental data play a crucial role in these elements in order to judge the quality of the calculations.

Chromium is of importance because of its high cosmic abundance and singly ionized chromium, as well as its spectrum Cr II, is prominent in a variety of astronomical objects. Among these objects is the massive star Eta Carinae which is used to identify numerous parity forbidden lines of the iron-group elements (Hartman et al. 2004; Bautista et al. 2009).

In astrophysical low-density plasma regions, the time-scale of collisional de-excitation is of the same order as the spontaneous radiative decay through forbidden transitions. The spectral lines associated with these transitions are therefore sensitive to the density and temperature of the surroundings, and they can serve as tools for measurements of these quantities provided that the

radiative decay rates (A-values) are known. One way to determine the rates is by combining the lifetime of the upper level with the branching fractions (BFs) of the different decays from the same level. We have developed a technique in which metastable lifetimes, measured using a laser-probing technique on a stored ion beam, are combined with BFs from astrophysical spectra. Individual A-values can then be derived. This has successfully been applied to a number of elements (see e.g. Hartman et al. 2005; Gurell et al. 2009).

Furthermore, the need for accurate atomic data for Cr II has also been pointed out by Dimitrijevic et al. (2007) for stellar abundance studies and by Wasson, Ramsbottom & Norrington (2010) for calculation of collision strengths.

2 ION STORAGE RING EXPERIMENT WITH Cr II

The storage ring CRYRING (Schuch et al. 1989) at Stockholm, Sweden, consists of 12 straight sections with bending magnets in between, which gives a total circumference of 50 m. A hot cathode ion source of Nielsen type (Nielsen 1957) mounted before an isotope separating $90°$ bending magnet produced single charged chromium ions which were accelerated to 42 keV prior to injection into the ring. Once inside the ring the ions circulated in an ambient ultrahigh vacuum below 10^{-11} mbar, which allows the ion beam to be stored for several minutes.

⋆E-mail: erba@physto.se

The ion source was loaded with Cr_2Cl_3 and heated to temperatures above 400°C to produce Cr^+ ions. An ion beam current of around 1.5 µA was obtained and a fraction of the ions were in the metastable state of interest.

2.1 Laser probing of the $c^4D_{5/2,7/2}$ levels

A laser-probing technique (Lidberg et al. 1999; Mannervik et al. 2005) has been developed at Stockholm University and refined during the last decade. It has been proved useful in determining lifetimes from milliseconds (3.4 ms in Xe II; Lidberg et al. 1997) to minutes (89 s in Ba II; Gurell et al. 2007). Instead of passively monitoring the decay of the population in the metastable state, it is actively probed using a tunable CW laser. In one of the straight sections a Doppler tuning device (DTD) is installed. The DTD locally accelerates the ions and the corresponding Doppler shift allows the ions to be in resonance with the laser light in the middle of the DTD. The local change in velocity will keep the ions in resonance with the laser light for approximately 1 cm and the ions in the c^4D metastable state will be pumped promptly to the higher lying $z\,^4D°$ state. An allowed transition from the upper level then produces fluorescent light which is detected by a photomultiplier tube in this area.

Energy levels and schematics of the laser probing can be seen in Fig. 1 along with relevant A-values involved in the probing. These are obtained from Kurucz (1988) and Martin, Fuhr & Weise (1988).

The fluorescent light intensity is directly proportional to the population in the metastable state and by probing at different delays after ion injection, a decay curve is recorded. A new sample of ions has to be inserted into the ring after each probe pulse since the probing depletes the population in the metastable state. The initial population in the metastable state may vary from sample to sample. If such variations occur it is important to compensate for these in order to obtain accurate values. By probing every fourth ion sample at a fixed time after injection, we are able to monitor the fluctuations in the initial population of the metastable state during the course of the experiment. Normally the variations are small, often negligible, as no significant trends in the initial population were observed.

The desired probing wavelengths of 6047 Å for the $J = 7/2 \rightarrow J = 7/2$ level and 6064 Å for the $J = 5/2 \rightarrow J = 7/2$ level could be obtained with a Coherent 699-29 ring dye laser with rhodamine 6G as gain medium. The dye laser was pumped with a Coherent Innova argon ion laser. At stable operation, it produced an irradiance of 180 mW, which was guided into the ring through a series of mirrors and a telescope.
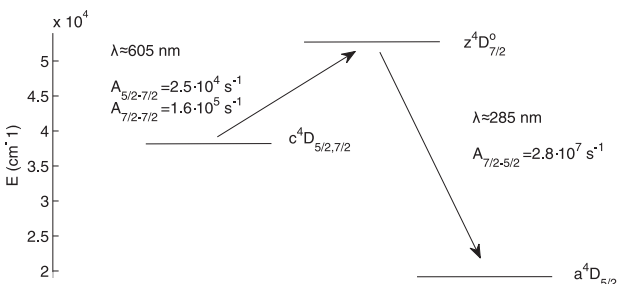
Figure 1. Energy-level diagram and A-values for some of the relevant transitions.

3 ANALYSIS

The recorded data (i.e. fluorescent light) from a complete probing cycle include systematic effects that have to be corrected for. The uncertainty in the estimation of these effects together with the statistical uncertainty of the initial population and the statistical Poisson error of photon counting contributes to the total uncertainty in the recorded data. Systematic effects arising from ion beam collision processes with the remaining gas in the ring have to be considered. The analysis of these effects is explained in detail in the sections below.

At base pressure, the vacuum inside the ring is below the range of the vacuum meters (10^{-11} mbar). In order to estimate the pressure dependence of the measured lifetimes, data sets collected at different pressures are compared. This can be achieved by heating one of the non-evaporate getter (NEG) pumps and thereby raising the pressure in the ring. A total of five data sets were collected at each pressure for the $J = 7/2$ level and then added in order to obtain better statistics. In the same way, eight measurements were made at the low pressure and four at the higher pressure for the $J = 5/2$ level and then added. The difference in the intensity of the collected light between the two levels can partly be ascribed to differences in the A-values of the transitions involved. Each data set contained 20 data points corresponding to probing with 150 ms delays. The poor signal, particularly for the $D_{5/2}$ level, reduced the best-fitting region to the first 11 points, which is roughly 1.5 times the measured lifetime.
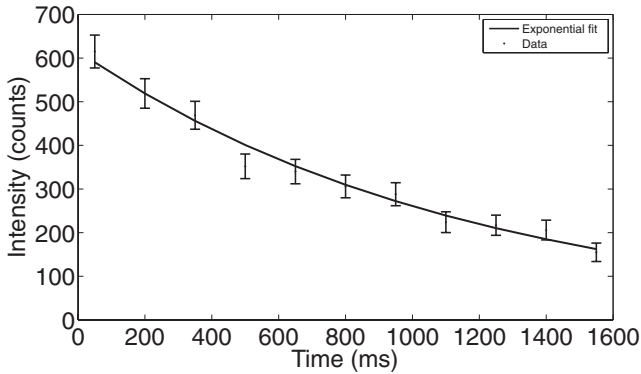
3.1 Repopulation

The process of the collisional excitation of ground state ions into the metastable state, hereby referred to as repopulation, has been identified as a systematic effect that needs to be considered in most cases. The effect of repopulation of the metastable state manifests itself as a larger signal than expected from probing at times later than the intrinsic lifetime of the metastable state. Since the state is repopulated the number of ions in the metastable state, and hence the recorded signal, does not approach zero with time; rather it approaches a constant steady-state value. This effect can be substantial. In fact, measuring the repopulation may be sufficient for determining the lifetime of the state (Royen et al. 2007). In our experiment the effect is negligible for the $c^4D_{5/2}$ level (i.e. the signal was below the background signal of ≈5 counts s^{-1}). For the $c^4D_{7/2}$ level, a repopulation effect could be observed. When correcting for the repopulation, the background automatically gets subtracted and hence the result reflects the radiative decay of the ion. The recorded and repopulation-corrected lifetime curves for the measured levels can be seen in Figs 2 and 3, together with the result of a least-squares fit of a first-order polynomial to the logarithm of the data. The exponential decay from the result of the fit determines the lifetime and the error of the lifetime is the (error propagated) standard least-squares error from the fit.

The effect of repopulation of the metastable state depends on the total number of stored ions in the ground state. Since a new ion beam is injected at every probing, the variation in the number of stored ions is monitored. By comparing the number of neutralized ions impinging on a multi-channel plate (MCP) detector at the same delay time after ion injection, it is possible to normalize the repopulation data against fluctuations in stored ions. The MCP is installed after one of the bending magnets, thereby all ions neutralized in the preceding straight section hit the detector. The amount of
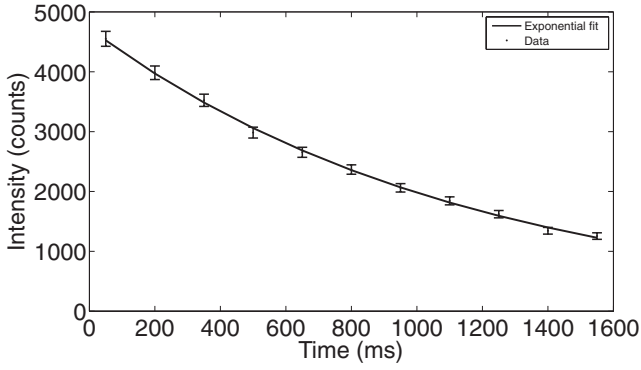
Figure 2. Recorded lifetime curve of the $c^4D_{7/2}$ level after systematic corrections.

Figure 3. Recorded lifetime curve of the $c^4D_{5/2}$ level after systematic corrections.

neutralized ions is assumed to be directly proportional to the total number of stored ions.

3.2 Collisional quenching

Not only repopulation but also collisional de-excitation may occur due to the gas remaining in the ring. This will quench the metastable state population. The collisional decay rate of the metastable level is assumed to be directly proportional to the pressure in the ring. The pressure in the ring is, however, below the range of the vacuum gauges and cannot be measured directly; instead the decay of the ion beam is monitored by detecting neutral particles on the MCP.

This decay rate is used as a relative measure of the pressure. By plotting the different metastable-level decay rates versus the ion beam decay rates in a Stern–Volmer plot (Demtröder 1998) and extrapolating to zero pressure, we can obtain the pure radiative decay. A minimum of two different measurements at different pressures are therefore needed. As mentioned above, this was achieved by heating one of the NEG pumps for a measurement at an increased pressure in addition to a measurement at the best possible vacuum at less than 10^{-11} mbar. A Stern–Volmer plot of the two different levels can be seen in Figs 4 and 5, respectively. The error in the pure radiative lifetime is then the error from the least-squares fit in the Stern–Volmer plot.

4 RESULTS AND DISCUSSION

The published theoretical values and the new experimental result can be seen in Table 1. The difference in the lifetime error estimation
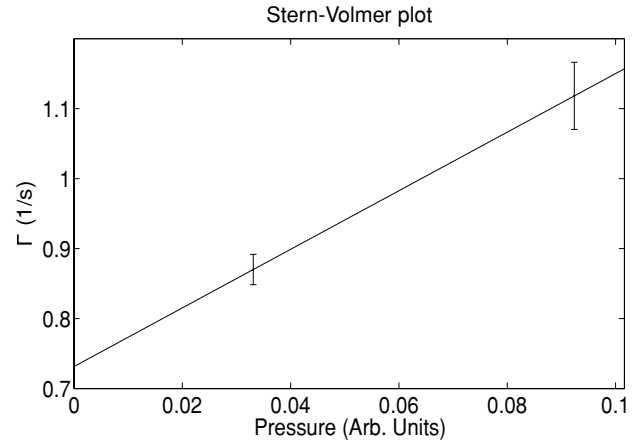
Figure 4. A Stern–Volmer plot of the $c^4D_{7/2}$ level. The pure radiative decay rate can be extracted from the intercept at zero pressure.
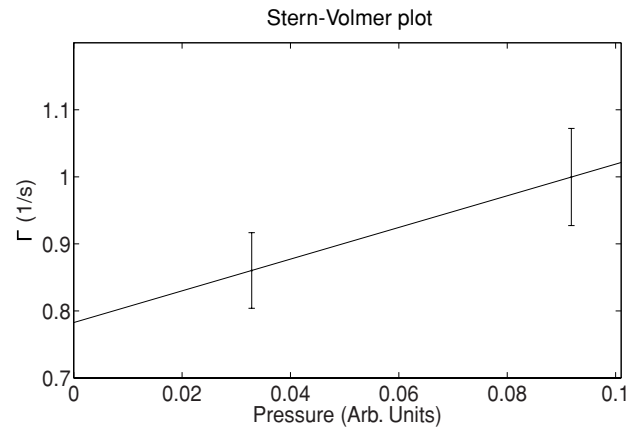
Figure 5. A Stern–Volmer plot of the $c^4D_{5/2}$ level. The pure radiative decay rate can be extracted from the intercept at zero pressure.

Table 1. Result of this experiment together with previous theoretical work.

| | | | τ (s) | |
Configuration	Term	Exp.	Ref.[a]	Ref.[b]
$3d^4(a^3D)4s$	$c^4D_{7/2}$	1.37 (7)	1.33	1.61
$3d^4(a^3D)4s$	$c^4D_{5/2}$	1.28 (16)	1.38	1.52

[a]Quinet (1997); [b]Nussbaumer & Swings (1970).

for the different levels originates from the exponential fit of the corrected data, as seen in Figs 2 and 3. The number of counts in the first data point is one order of magnitude higher for the $J = 7/2$ level, which gives a better exponential fit. This can also be seen in the Stern–Volmer plots where the error bars for the lifetimes from the $J = 7/2$ measurements are smaller than those for the $J = 5/2$ measurements. The straight line fit is hence more accurate for the $J = 7/2$ level. The next step would be to obtain BFs for these levels in order to deduce A-values for the transitions involved. Emission lines from these levels have, however, not been observed so far.

Levels for which BFs have been measured are the $c^4P_{3/2}$ and $c^4P_{5/2}$ metastable levels. At present, this level is not accessible via probing by a dye laser; however, this would be a good candidate for future experiments involving frequency-doubled light.

The difference between the two calculations (Nussbaumer & Swings 1970; Quinet 1997) is most likely due to inclusion of the core polarization of the 3s subshell in Quinet (1997). The corresponding excitations of the 3s give rise to configuration state functions with an open 3s subshell and an additional 3d occupancy. This in turn gives new contributions to the transition integrals through 3s–3d transitions. It has been shown (Quinet & Hansen 1995) that this represents a strong 'branch' for the electric quadrupole transitions.

REFERENCES

Bautista M. A., Ballance C., Gull T. R., Hartman H., Lodders K., Martinez M., Melendez M., 2009, MNRAS, 393, 1503

Demtröder W., 1998, Laser Spectroscopy, 2nd edn. Springer-Verlag, Berlin

Dimitrijevic M. S., Ryabchikova T., Simic Z., Popovic L. C., Dacic M., 2007, A&A, 469, 681

Fischer C. F., 2009, Phys. Scr., T134, 014019

Gurell J. et al., 2007, Phys. Rev. A, 75, 1

Gurell J., Hartman H., Blackwell-Whitehead R., Nilsson H., Bäckström E., Norlin L. O., Royen P., Mannervik S., 2009, A&A, 508, 525

Hartman H., Gull T., Johansson S., Smith N., HST Eta Carinae Treasury Project Team, 2004, A&A, 419, 215

Hartman H., Johansson S., Lundberg H., Lundin P., Mannervik S., Schef P., 2005, Phys. Scr., T119, 40

Johansson S. et al., 2002, Phys. Scr., T100, 71

Kurucz R. L., 1988, in McNally M., ed., Trans. IAU, XXB. Kluwer, Dordrecht, p. 168

Lidberg J., Al Khalili A., Cowan R. D., Norlin L.-O., Royen P., Mannervik S., 1997, Phys. Rev. A, 56, 2692

Lidberg J., Al Khalili A., Norlin L.-O., Royen P., Tordoir X., Mannervik S., 1999, Nucl. Instrum. Methods Phys. Res. B, 152, 157

Mannervik S., Ellmann A., Lundin P., Norlin L.-O., Rostohar D., Royen P., Schef P., 2005, Phys. Scr., T119, 49

Martin G. A., Fuhr J. R., Wiese W. L., 1988, J. Phys. Chem. Ref. Data, 17, Suppl. 3, 512

Nielsen K. O., 1957, Nucl. Instrum., 1, 289

Nussbaumer H., Swings J. P., 1970, AJ, 162, 509

Quinet P., 1997, Phys. Scr., T55, 41

Quinet P., Hansen J. E., 1995, J. Phys. B, 28, L213

Royen P., Gurell J., Lundin P., Norlin L.-O., Mannervik S., 2007, Phys. Rev. A, 76, 030502

Schuch R., Barany A., Danared H., Elander N., Mannervik S., 1989, Nucl. Instrum. Methods Phys. Res. B, 43, 411

Wasson I. R., Ramsbottom C. A., Norrington P. H., 2010, A&A, 524, A35

This paper has been typeset from a TEX/LATEX file prepared by the author.